

# Insight into the binding interaction of kaempferol-7-O- $\alpha$ -L-rhamnopyranoside with human serum albumin by multiple fluorescence spectroscopy and molecular modeling

WENTING ZHANG<sup>1\*</sup>, CHUN CHEN<sup>2\*</sup>, CHUNPING ZHANG<sup>2</sup>, JINGYU DUAN<sup>2</sup>,  
HUANKAI YAO<sup>2,3</sup>, YAN LI<sup>2</sup>, AIGUO MENG<sup>1</sup> and JUN SHI<sup>1</sup>

<sup>1</sup>Department of Laboratory Medicine, Hospital and School of Clinical Medicine, North China University of Science and Technology, Tangshan, Hebei 064000; <sup>2</sup>School of Pharmacy and Jiangsu Key Laboratory of New Drug Research and Clinical Pharmacy, Xuzhou Medical University, Xuzhou, Jiangsu 221004;

<sup>3</sup>Faculty of Health Sciences, University of Macau, Taipa, Macau SAR, P.R. China

Received January 10, 2016; Accepted February 3, 2017

DOI: 10.3892/etm.2017.4427

**Abstract.** Human serum albumin (HSA) is a transporting protein that has multiple functions. The binding interaction between HSA and small molecules affects its function and efficacy of small molecules. The present study reports that kaempferol-7-O- $\alpha$ -L-rhamnopyranoside (KR) interacts with HSA as indicated by multiple fluorescence spectroscopy and molecular modeling. KR can quench the intrinsic fluorescence of HSA through the formation of a KR-HSA complex in a static manner. In addition, the binding site is located in subdomain IIA as confirmed by competitive experiments using site-specific warfarin and ibuprofen, and the driving forces include hydrogen bonds, van der Waals forces and electrostatic interaction derived from a thermodynamic analysis. The formation of KR-HSA is exothermic and spontaneous. Although there is no hydrophobic interaction around Tyr and Trp residues, the secondary structure of HSA changes through the formation of the KR-HSA complex. In addition, docking results visualized and further supported these results. Finally, these results can provide more information to further investigate the use of KR on the prevention of diabetic complications.

## Introduction

Human serum albumin (HSA) is a 585 amino acid residue protein. In the plasma it is found at high concentrations of  $\sim 600 \mu\text{M}$  and can transport many endogenous and exogenous substances, including drugs, nutrients, toxins and hormones (1). Chemicals can bind HSA to maintain a stable concentration and lifetime in the plasma. Glycated HSA is one of the major advanced glycation end-products (AGEs) in diabetic patients and results in diabetic complications (2). Furthermore, it is a biomarker that is used to predict the control of blood glucose in diabetic patients (3). Small molecules usually inhibit the formation of AGEs derived from HSA through binding interaction and intervention in the non-enzymatic reactions, including oxidation and cross-linking (4). Phytochemicals, particularly polyphenols are important in the discovery of AGEs formation inhibitors, which may inhibit the formation of AGE (5,6). Furthermore, studies on the binding interaction between quercetin and HSA are essential to evaluate quercetin on inhibiting the formation of glycated HSA (5).

The structure of HSA can be divided into three similar domains (I-III) and each includes two subdomains (A and B). For the majority of the chemicals, two primary binding sites (sites I and II) are located in subdomains IIA and IIIA, respectively. In subdomain IIA, there is a unique tryptophan residue (Trp214) that emits fluorescence following excitation (7). Although Trp, tyrosine (Tyr) and phenylalanine (Phe) residues of HSA can contribute to the fluorescence, only Trp214 has intrinsic fluorescence due to the low quantum yield of the Phe residue and the effects of ionization and some functional groups on the Tyr residue (8).

Kaempferol-7-O- $\alpha$ -L-rhamnopyranoside (KR) is a natural flavonoid found in numerous plants, including *Streblus asper* (9), *Cardamine leucantha* (10) and *Cyclocarya paliurus* (11). KR can inhibit lipopolysaccharide-induced production of nitric oxide in RAW 264.7 macrophages and reduce prostaglandin E2 accumulation as the anti-inflammatory agent (12). In order to search for the bioactive phytochemicals attenuating diabetic nephropathy, KR has been previously identified in

---

*Correspondence to:* Dr Huankai Yao, School of Pharmacy and Jiangsu Key Laboratory of New Drug Research and Clinical Pharmacy, Xuzhou Medical University, 209 Tongshan Road, Xuzhou, Jiangsu 221004, P.R. China  
E-mail: hkyao@xzhmu.edu.cn

Professor Jun Shi, Department of Laboratory Medicine, Hospital and School of Clinical Medicine, North China University of Science and Technology, 73 North Jianshe Road, Tangshan, Hebei 064000, P.R. China  
E-mail: shijunts@163.com

\*Contributed equally

**Key words:** flavonoid, human serum albumin, binding interaction, fluorescence spectroscopy, molecular modeling

the Chinese medicinal fern *Polypodium hastatum*, which showed antioxidative activity (13,14). Herein we report the interaction between HSA and KR, evaluated using multiple fluorescence spectroscopy and molecular modeling.

## Materials and methods

**Chemicals and reagents.** The water was prepared using a Milli-Q system (EMD Millipore, Billerica, MA, USA). HSA, warfarin, ibuprofen and Tris were purchased from Sigma-Aldrich (Sigma-Aldrich; Merck KGaG, Darmstadt, Germany). The other reagents were of analytical grade.

**Preparation of HSA and drug solutions.** Tris was dissolved in water to a concentration of 0.05 M, and was calibrated to pH 7.4 with hydrochloric acid. Next, HSA was added into Tris-HCl solution to make a solution at a concentration of  $1.0 \times 10^{-5}$  M. Warfarin and ibuprofen were dissolved in dimethyl sulfoxide (DMSO) to obtain  $5.0 \times 10^{-3}$  M solutions, respectively. In addition, KR solution was prepared with DMSO at  $3.0 \times 10^{-3}$  M.

**Fluorescence spectroscopy.** In this experiment, KR solution was gradually added to the HSA solution to increase its concentration from 0 to  $3.0 \times 10^{-5}$  M at increments of  $0.3 \times 10^{-5}$  M. The fluorescence spectra were recorded using an L55 fluorescence spectrometer (PerkinElmer, Inc., Waltham, MA, USA) at 298, 304 and 310 K. Furthermore, the excitation wavelength was 290 nm and the emission wavelength was between 300 and 450 nm.

**Identification of a binding site.** To identify the binding site of KR with HSA, a competitive experiment with site markers has been implemented. In the mixed solution with equal quantities of HSA and site marker, the KR solution was gradually added at increments of  $0.3 \times 10^{-5}$  M. In addition, the fluorescence intensities were determined.

**Synchronous fluorescence spectroscopy.** To study the characteristics of intrinsic Tyr and tryptophan residues, synchronous fluorescence spectroscopy was employed. The excitation and emission slit widths were set at 5 and 10 nm, respectively. Furthermore, the concentrations of HSA were adjusted to  $1.5 \times 10^{-6}$  and  $0.15 \times 10^{-6}$  M according to the varied scanning intervals ( $\Delta\lambda$ ) at 15 and 60 nm. Next, the spectra of HSA were recorded upon the titration of KR from 0 to  $1.8 \times 10^{-5}$  M.

**Three-dimensional (3D) fluorescence spectroscopy.** The excitation and emission slit widths were set at 10 and 5 nm, respectively. The emission spectra were recorded from 260 to 450 nm with an excitation wavelength range between 220 and 450 nm, and with a 5-nm interval. Furthermore, the concentration of HSA was  $0.6 \times 10^{-6}$  M, and the ratios of KR and HSA were 0:1 and 10:1, respectively.

**Molecular modeling.** The structure of KR was generated as the ligand using SYBYL software, version X2.1 (Certara USA, Inc., Princeton, NJ, USA) on a Windows 7 workstation and minimized using a Tripos force field. Furthermore, the HSA

crystal file was obtained from the RCSB Protein Data Bank (Protein Data Bank code: 2BXD). After the water was removed from the crystal structure, hydrogens and charges were added. Next, docking was performed by the Surflex-Dock module.

## Results

**Fluorescence quenching and mechanism.** As shown in Fig. 1, the HSA can emit fluorescence without KR. The fluorescence intensity decreased gradually following the addition of KR solution, which indicated that fluorescence quenching occurred. At the same time, the maximum emission wavelength showed a slight 'blue shift' from 339 to 337 nm (demonstrated when the peak moves towards the short wave length). The quenching can be analyzed by the Stern-Volmer equation (i) at different temperatures:  $F_0/F = 1 + K_{sv}[Q]$ ; in which  $F_0$  and  $F$  are the fluorescence intensity with or without quencher.  $K_{sv}$  represents the quenching constant and  $[Q]$  is the concentration of quencher. Hence,  $K_{sv}$  can be derived from the linear regression of  $(F_0 - F)/F$  vs.  $[Q]$ .

Fluorescence quenching can be classified as static and dynamic quenching based on the response to temperature. As the  $K_{sv}$  value decreases following the increasing temperature, the quenching between KR and HSA is static.

**Identification of the binding site.** For the static quenching, the ligand will be bound to HSA to form a complex. Furthermore, the binding site can be identified using the double logarithm equation (ii):  $\log(F_0 - F)/F = \log K + n \log [Q]$ ; where  $F_0$  and  $F$  are the fluorescence intensities of protein in the absence and presence of ligand, respectively.  $K$  is the binding constant;  $n$  is the number of binding sites and  $[Q]$  is the concentration of quencher. As shown in Table I, the values of  $n$  are close to 1 at different temperatures. Additionally,  $K$  values decrease following the increasing temperature, which is in accordance with the  $K_{sv}$  values.

To further confirm the binding site of KR, a competitive experiment was implemented with specific markers, warfarin and ibuprofen. After the addition of warfarin, the maximum emission wavelength presented an evident 'red shift' from 339 to 359.5 nm (demonstrated when the peak moves towards the long wave length) and the fluorescence intensity of HSA descended (Fig. 2A). However, the fluorescence quenching was weaker than ibuprofen when KR was added. In the presence of ibuprofen, the fluorescence of HSA was not affected and the quenching was evident after the addition of KR (Fig. 2B).

**Thermodynamic analysis.** To elucidate the binding forces between KR and HSA, the Van't Hoff equation (iii) was employed in thermodynamic analysis:  $\ln K = -\Delta H/RT + \Delta S/R$ ; where  $K$  is the binding constant at a respective temperature, and  $R$  is the gas constant.  $\Delta H$  and  $\Delta S$  are the changes of enthalpy and entropy, respectively. The thermodynamic parameters of the KR-HSA system were calculated from the Van't Hoff plot of  $\ln K$  against  $1/T$ . In addition, the driven force can be expressed by the Gibbs free energy change ( $\Delta G$ ) and obtained from the following equation (iv):  $\Delta G = \Delta H - T\Delta S$ .

As shown in Table I,  $\Delta H$ ,  $\Delta S$  and  $\Delta G$  values are negative, which indicates that the interaction is exothermic and

Table I. Quenching and thermodynamic parameters for the interaction of kaempferol-7-O- $\alpha$ -L-rhamnopyranoside with human serum albumin.

pH	T (K)	KSV ( $10^5 \text{ M}^{-1}$ )	Kb ( $10^6 \text{ M}^{-1}$ )	n	$\Delta H$ (kJ/mol)	$\Delta S$ (J/mol)	$\Delta G$ (kJ/mol)
7.4	298	1.37	3.76	1.33	-38.73	-3.45	-37.71
	304	1.29	3.49	1.32			-37.68
	310	1.27	2.05	1.28			-37.66

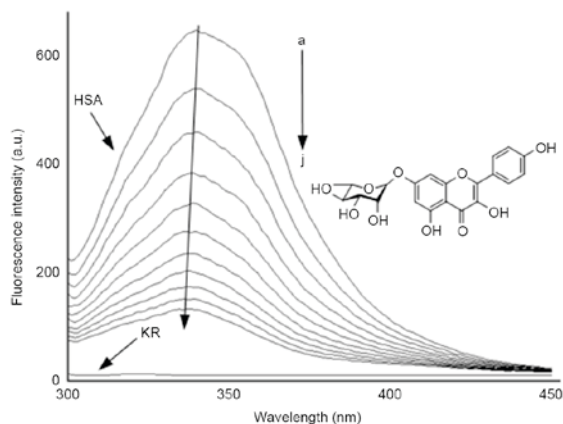


Figure 1. Interaction between KR and human serum albumin at 298 K and pH 7.4. (a to j): 0 to  $3.0 \times 10^{-5}$  M. HSA, human serum albumin; KR, kaempferol-7-O- $\alpha$ -L-rhamnopyranoside.

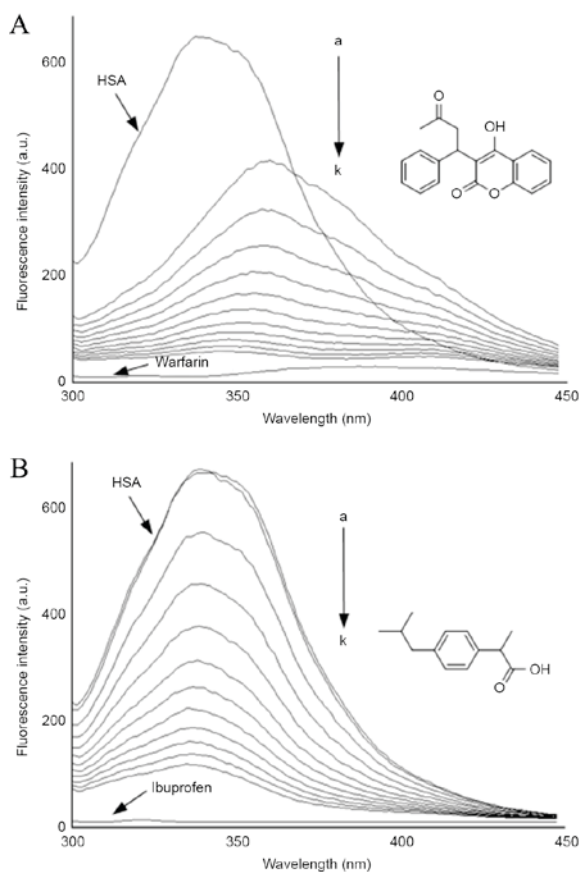


Figure 2. Effects of site markers on the spectra of human serum albumin. (A) Warfarin and (B) ibuprofen. (a to k): 0 to  $3.0 \times 10^{-5}$  M. a.u., absorbance units; HSA, human serum albumin.

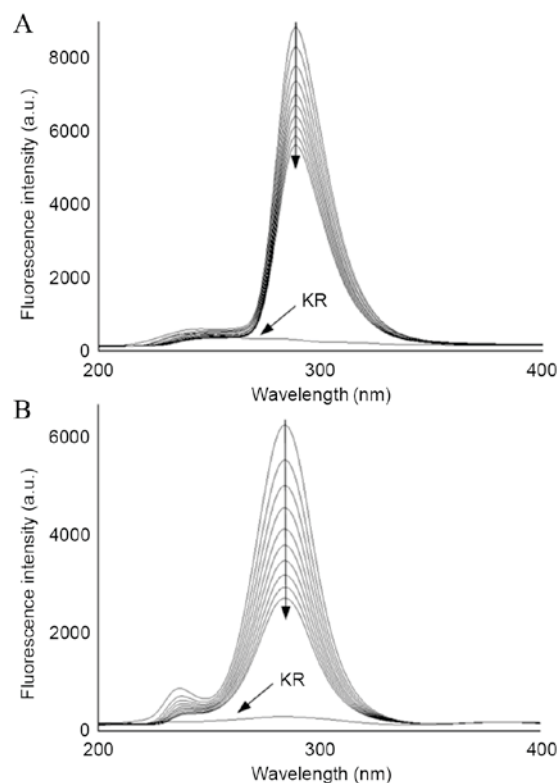


Figure 3. Synchronous fluorescence spectra of human serum albumin. (A)  $\Delta\lambda=15$  nm and (B)  $\Delta\lambda=60$  nm. a.u., absorbance units; KR, kaempferol-7-O- $\alpha$ -L-rhamnopyranoside.

spontaneous. In addition, the values of  $\Delta G$  decrease according to the increasing temperature, which demonstrates the binding interaction weakens accordingly.

**Synchronous fluorescence spectroscopy.** Synchronous fluorescence spectroscopy can describe the microenvironment of Tyr and Trp as the wavelength differences ( $\Delta\lambda$ ) between the excitation and emission wavelength were fixed at 15 and 60 nm, respectively. As in Fig. 3, when the addition of KR was initialized, fluorescence quenching appeared but the maximum wavelength ( $\lambda_m$ ) remained at 289 and 284 nm respectively.

**3D fluorescence spectroscopy.** 3D fluorescence spectroscopy is a tool used to investigate the conformational changes of proteins. As shown in Fig. 4, there was a weak peak ( $\lambda_{ex}=\lambda_{em}$ ) caused by Rayleigh scattering. In the presence of KR at the molar ratio of 10:1, the 3D fluorescence spectrum of HSA changed evidently. The intensity of peaks I and II dropped greatly following the fluorescence quenching, particularly of peak I.



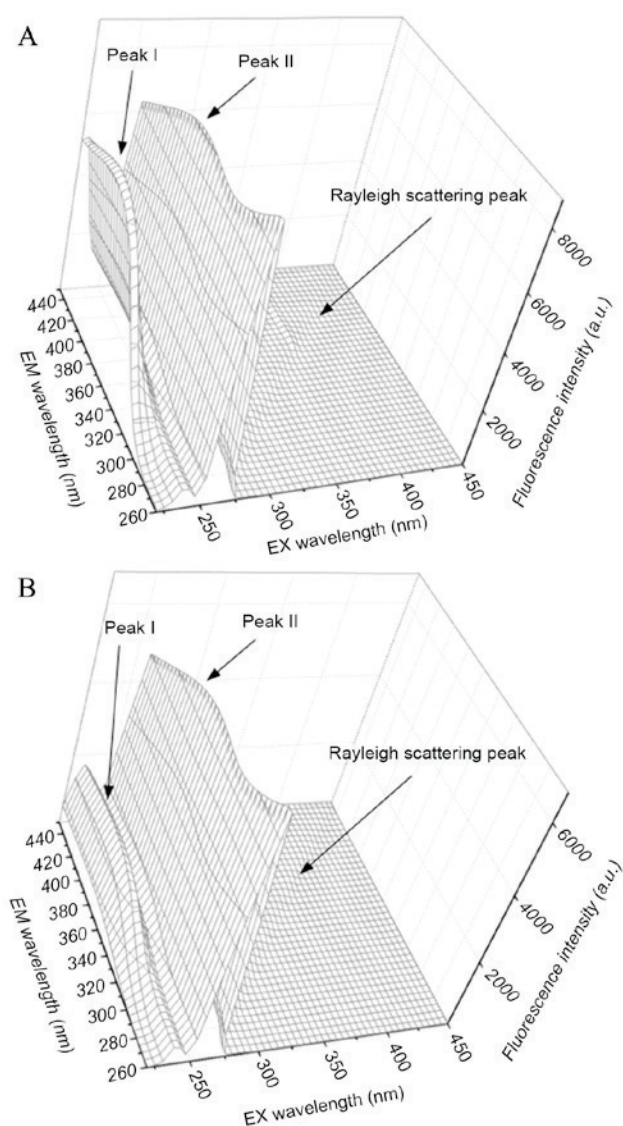


Figure 4. Three-dimensional fluorescence spectra of human serum albumin. (A) In absence and (B) in presence of kaempferol-7-O- $\alpha$ -L-rhamnopyranoside. a.u., absorbance units; EM, emission; EX, excitation.

**Molecular modeling.** Molecular modeling can visualize the detailed interaction between KR and HSA. KR can enter the cavity of subdomain IIA and interact through hydrogen bonds with Glu153 (1.9 Å), Lys199 (2.2, 2.8 Å), Arg257 (1.9, 2.1, 2.1 Å), His288 (2.6 Å) and Glu292 (2.1 Å). The total score of KR (7.49) is similar to warfarin (7.41). KR in site I is near the Trp-214 and affects the microenvironment around the fluorescence quenching (Fig. 5A). A 2D interaction diagram shows there are van der Waals forces, Pi and electrostatic interactions besides the hydrogen bonds (Fig. 5B). In detail KR can interact with the residues of HSA, including Tyr150, Phe156, Phe157, Glu188, Ser192, Trp214, Arg222, Leu219, Phe223, Leu238, Leu260, Ala258, Ala261, Ser287 and Val241 through van der Waals forces. Furthermore, Pi interaction occurs between the 3-phenylchromone scaffold of KR and both the His242 and Ala291 residues. In addition, an electrostatic interaction can be found between KR and the Glu153, Lys195, Lys199, Arg257, His288 and Glu292 residues.

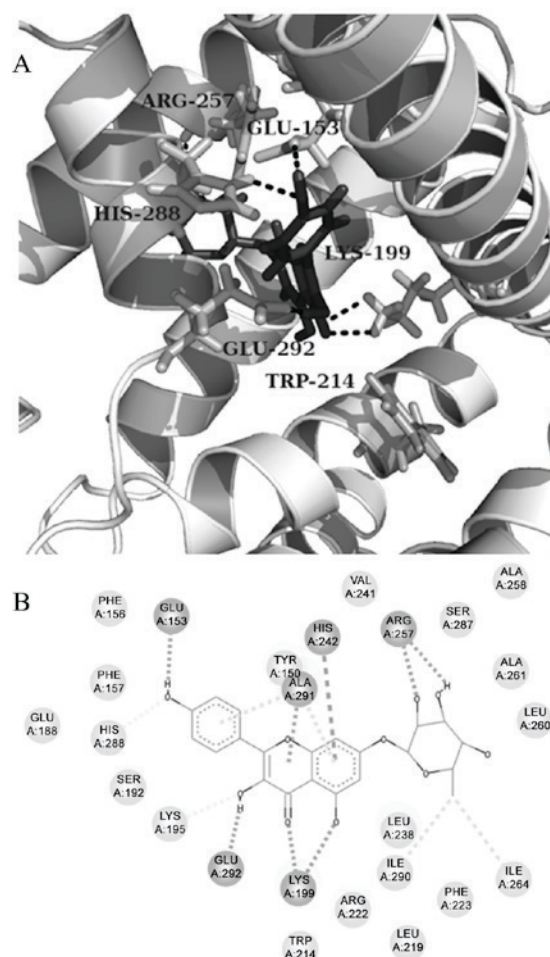


Figure 5. Molecular modeling for the binding interaction between KR and HSA. (A) Binding pose of KR (in black) in site I with hydrogen bonds (black dash) and relative position to Trp-214 (in gray); (B) two-dimensional interaction diagram of KR and HSA. The dash lines between KR and residues Glu153, Lys199, Arg257, His288 and Glu292 represent hydrogen bonds; the dash lines between KR and His242 as well as Ala291 illustrate the pi interaction. KR, kaempferol-7-O- $\alpha$ -L-rhamnopyranoside; HSA, human serum albumin.

## Discussion

If a ligand interacts with HSA, fluorescence quenching may appear due to the change of microenvironment around the fluorophores, particularly Trp214. The quenching can be divided as static and dynamic according to the response to temperature. The former is related to formation of a ligand-HSA system and the latter to collision. Furthermore, KR can induce the quenching in the spectra of HSA at different temperatures. In addition, the values of  $K_{sv}$  decrease following increasing temperatures, which demonstrates it is static quenching and there is a KR-HSA complex in the solution. The values of  $K$  and  $\Delta G$  further support this conclusion. The static quenching also indicates that the main binding site is located in site I for the unique Trp214 is in subdomain IIA. Competitive experiments with site markers back up the indication as the fluorescence spectra of HSA with or without KR were not affected in the presence of ibuprofen but warfarin can impact the spectra.

The driving forces of the interaction can be derived from thermodynamic analysis. The negative  $\Delta H$  and  $\Delta S$  imply there are hydrogen bonds, van der Waals forces and electrostatic interactions contributing to the formation of the KR-HSA complex according to the description by Ross and Subramanian (15). Additionally, negative  $\Delta G$  shows that the binding is exothermic and spontaneous.

For the synchronous fluorescence spectra that can elucidate the microenvironments surrounding the Tyr and Trp residues, the steady maximum wavelength demonstrates that there are no changes for the hydrophobicity and polarity around Tyr and Trp. In the 3D fluorescence spectrum of HSA, peak II is associated to the spectral behavior of Tyr and Trp residues as well as peak I to peptide backbones (16). Compared to the 3D spectrum of HSA, the intensities of peaks I and II in the 3D spectrum of HSA with KR decreased, particularly peak I. These results indicate that KR in site I is close to the Tyr and Trp residues and affects their spectral behavior. In addition, the decreased intensity of peak I implicates that KR can cause conformational changes of HSA through varying the helices surrounding it. Furthermore, the 3D spectra reveal the formation of a KR-HSA complex that can affect the secondary structure of HSA, and KR can access the Tyr and Trp residues.

Molecular modeling is a potent tool used to visualize molecular interaction. The docking results present the detailed driving forces that form the KR-HSA complex. These forces include hydrogen bonds, van der Waals forces,  $\pi$  and electrostatic interactions. However, no hydrophobic interaction is detected even though the interaction occurs in solution. These results are in accordance with the conclusion from the experiments described above.

## Acknowledgements

The present study was partly funded by the National Natural Sciences Foundation of China (grant nos. 81302744 and 31300222), the Scientific Research Foundation for the Returned Overseas Chinese Scholars of State Education Ministry, the Natural Sciences Foundation of Jiangsu Province (grant no. BK20130214) and the Natural Sciences Foundation of the Colleges and Universities in Jiangsu Province (grant no. 13KJB180025), and the authors gave sincere gratitude to those institutions.

## References

1. Trainor GL: The importance of plasma protein binding in drug discovery. *Expert Opin Drug Dis* 2: 51-64, 2007.
2. Anguizola J, Matsuda R, Barnaby OS, Hoy KS, Wa C, DeBolt E, Koke M and Hage DS: Review: Glycation of human serum albumin. *Clin Chim Acta* 425: 64-76, 2013.
3. Zheng CM, Ma WY, Wu CC and Lu KC: Glycated albumin in diabetic patients with chronic kidney disease. *Clin Chim Acta* 413: 1555-1561, 2012.
4. Peyroux J and Sternberg M: Advanced glycation endproducts (AGEs): Pharmacological inhibition in diabetes. *Pathol Biol (Paris)* 54: 405-419, 2006.
5. Alam MM, Ahmad I and Naseem I: Inhibitory effect of quercetin in the formation of advanced glycation end products of human serum albumin: An in vitro and molecular interaction study. *Int J Biol Macromol* 79: 336-343, 2015.
6. Ito H, Li P, Koreishi M, Nagatomo A, Nishida N and Yoshida T: Ellagitannin oligomers and a neolignan from pomegranate arils and their inhibitory effects on the formation of advanced glycation end products. *Food Chem* 152: 323-330, 2014.
7. Sudlow G, Birkett DJ and Wade DN: The characterization of two specific drug binding sites on human serum albumin. *Mol Pharmacol* 11: 824-832, 1975.
8. Hua T and Liu Y: Probing the interaction of cefodizime with human serum albumin using multi-spectroscopic and molecular docking techniques. *J Pharm Biomed Anal* 107: 325-332, 2015.
9. Chen H, Li J, Wu Q, Niu XT, Tang MT, Guan XL, Li J, Yang RY, Deng SP and Su XJ: Anti-HBV activities of *Streblus asper* and constituents of its roots. *Fitoterapia* 83: 643-649, 2012.
10. Yang F, Su YF, Bi YP, Xu J, Zhu ZQ, Tu GZ and Gao XM: Three new kaempferol glycosides from *Cardamine leucantha*. *Helv Chim Acta* 93: 536-541, 2010.
11. Wu Y, Li YY, Wu X, Gao ZZ, Liu C, Zhu M, Song Y, Wang DY, Liu JG and Hu YL: Chemical constituents from *cyclocarya paliurus* (Batal.) Iljinsk. *Biochem Syst Ecol* 57: 216-220, 2014.
12. Lin HY and Chang ST: Kaempferol glycosides from the twigs of *Cinnamomum osmophloeum* and their nitric oxide production inhibitory activities. *Carbohydr Res* 364: 49-53, 2012.
13. Yao H, Duan J, Ai F and Li Y: Chemical constituents from a Chinese fern *Polypodium hastatum* Thunb. *Biochem Syst Ecol* 44: 275-278, 2012.
14. Duan J, Liu Y, Zhang C, Wei X, Zong Z, Yao H and Li Y: Flavonoids from the Chinese fern *Polypodium hastatum* Thunb. and relevant antioxidative activity. *Lat Am J Pharm* 33: 696-700, 2014.
15. Ross PD and Subramanian S: Thermodynamics of protein association reactions: Forces contributing to stability. *Biochemistry* 20: 3096-3102, 1981.
16. Lin J, Liu Y, Chen M, Huang H and Song L: Investigation on the binding activities of citalopram with human and bovine serum albumins. *J Lumin* 146: 114-122, 2014.